ENGINEERING RESEARCH INSTITUTE
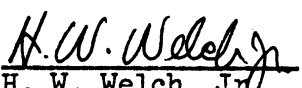UNIVERSITY OF MICHIGAN
ANN ARBOR

STUDY, DEVELOPMENT, AND PRODUCTION OF FERROSPINELS

APPLICABLE TO TUNING OF SEARCH RECEIVERS

QUARTERLY PROGRESS REPORT NO. 2, TASK ORDER NO. EDG-6
Period Covering January 1, 1953 to March 31, 1953

Electronic Defense Group
Department of Electrical Engineering

By: D. M. Grimes
    B. Hershenov
    E. Katz
    D. W. Martin
    L. Thomassen
    E. F. Westrum, Jr.
    M. H. Winsnes

Approved by: *H. W. Welch*
H. W. Welch, Jr.
Project Engineer

Project M-970

April, 1953

TABLE OF CONTENTS

LIST OF ILLUSTRATIONS

LIST OF TABLES

TASK ORDER

Title: STUDY, DEVELOPMENT, AND PRODUCTION OF FERROSPINELS APPLICABLE TO TUNING OF SEARCH RECEIVERS

Purpose of Task:

To further the development of ferrospinels of different incremental permeabilities and low losses, with reference to specific applications of interest to the Signal Corps such as RF tuning units.

Procedure:

The approach to the general objective will include:

a. The preparation, under controlled conditions, of specimens of of different compositions;

b. The measurement of parameters such as the incremental and initial permeabilities, the saturation inductance, the coercive force and the Q (figure of merit) at various frequencies;

c. The interpretation of these magnetic parameters in terms of the composition, reaction temperature, pressure and other conditions in the preparation of the samples;

d. The relationship of the solid state properties of the crystallite with the various measured magnetic parameters;

e. Theoretical explanations, where possible, for the relationships found in d. above.

Reports and Conferences:

a. Quarterly Task Order Reports shall be submitted reporting technical detail and progress under this Task Order;

b. Task Order Technical Reports of a final summary type are in general desirable and shall be prepared at the conclusion of investigations of each major phase. Such reports shall be prepared as

decided in conference between the Electronic Defense Group and the Contracting Officer's Technical Representative in the Countermeasures Branch, Evans Signal Laboratory.

Personnel:

Electronic Defense Group:

Project Physicist: Mr. D. M. Grimes

Countermeasures Branch, Evans Signal Laboratory:

Project Engineer: Mr. Leon I. Mond

Components and Materials Branch, Squier Signal Laboratory

Project Scientist: Dr. E. Both

Comments:

The classification of this Task Order as Unclassified shall not preclude the classification of individual reports according to the information they contain, as determined in conference with the Contracting Officer's Technical Representative.

M. KEISER
Chief, Countermeasures Branch
Contracting Officer's Technical
Representative

ABSTRACT

Susceptibility-magnetization curves on two ferrite samples are shown. The method of measurement is briefly described. The status of the manufacture of ferrite material is described. Specific heat data on a General Ceramics type E ferrite are shown, as are calculations of specific heat discontinuities for cores with the proper chemistry. Progress on the manufacture of suitable specimens for Hall Coefficient measurements is described.

STUDY, DEVELOPMENT, AND PRODUCTION OF FERROSPINELS

APPLICABLE TO TUNING OF SEARCH RECEIVERS

QUARTERLY PROGRESS REPORT NO. 2, TASK ORDER NO. EDG-6
Period Covering January 1, 1953 to March 31, 1953

1. PURPOSE

The purpose of this report is to summarize the progress made by Task Group 6 of the Electronic Defense Group from January 1, 1953 to March 31, 1953 on the Signal Corps Contract No. DA-36-039 sc-15358.

The purpose of the task is to further the development of ferrospinels of different incremental permeabilities and low losses, with reference to specific applications of interest to the Signal Corps such as r-f tuning units.

The proposed program of Task Group EDG-6 was outlined in the previous progress report. Only those items will now be reported which have been worked on during the period.

2. PUBLICATIONS AND REPORTS

No publications were issued during the quarter on Task Order No. EDG-6.

Mr. D. M. Grimes visited the Bell Telephone Laboratories, Murray Hill, New Jersey, and attended the solid state meeting of the American Physical Society in Durham, N. C.

3. FACTUAL DATA

3.1 Check of the Reversible Susceptibility Theory   (D. M. Grimes, M. H. Winsnes)

3.1.1 Reversible Susceptibility in Ferrimagnetic Materials. The expression for the parallel reversible susceptibility was given by Gans[1] in 1911. His parametric expressions,

$$\frac{\chi_{rp}}{\chi_o} = 3L'(\eta) \quad ; \quad \frac{J}{J_s} = L(\eta)$$

$$L(\eta) = \text{ctnh}\ \eta - \frac{1}{\eta}$$

where:

χ_{rp} is the parallel reversible susceptibility

χ_o is the initial susceptibility

J is the magnetization

J_s is the saturation magnetization

η is a parameter

fitted the experimental data quite well for a wide variety of materials. The equations were first derived by Brown[2] in 1938 using the classical Heisenberg model and a statistical approach utilizing some of the techniques of statistical mechanics. These equations can be obtained quite easily by the following argument:

Assume the Heisenberg model of N domains, all of fixed and equal volume, magnetized to saturation in some easy direction. When a magnetic field is applied the potential energy of each domain $U_i = \alpha\ J_s H \ell_i$ where:

α is a constant.

ℓ_i is the direction cosine between the directions of the field and the magnetization.

H is related to the applied field.

2

If n_i is the number of domains oriented in the particular direction i, $\sum_i n_i = N$. If one now assumes the number of domains oriented in each direction is proportional to $e^{-\beta U_i}$ where β is a constant with dimensions of inverse energy:

$$n_i = N \frac{e^{-\beta U_i}}{\sum_j e^{-\beta U_j}} \quad .$$

The macroscopic magnetization J is given by:

$$J = J_s \sum_i \ell_i n_i = J_s \frac{\sum_i \ell_i e^{-\beta U_i}}{\sum_j e^{-\beta U_j}} = J_s \frac{\sum_i \ell_i e^{-\beta \alpha J_s H \ell_i}}{\sum_j e^{-\beta \alpha J_s H \ell_j}} \quad .$$

If one now assumes isotropic material, so that the magnetization vectors can lie in any direction,

$$J = J_s \frac{\int_0^\pi \cos \Theta \sin \Theta \, d\Theta \, e^{-\beta \alpha J_s H \cos \Theta}}{\int_0^\pi \sin \Theta \, d\Theta \, e^{-\beta \alpha J_s H \cos \Theta}} \quad .$$

Now substitute:

$$\eta = \beta \alpha J_s H$$

$$\gamma = \cos \Theta$$

$$S = \int_{-1}^{1} d\gamma \, e^{-\eta \gamma}$$

$$J = J_s \frac{\frac{dS}{d\eta}}{S}$$

$$S = \frac{1}{\eta} \left[e^\eta - e^{-\eta} \right]$$

$$\frac{dS}{d\eta} = \frac{1}{\eta} \left[e^\eta + e^{-\eta} \right] - \frac{1}{\eta^2} \left[e^\eta - e^{-\eta} \right]$$

$$\frac{J}{J_s} = \operatorname{ctnh} \eta - \frac{1}{\eta}$$

3

Upon differentiating this with respect to H,

$$\frac{X_{rp}}{X_o} = 3 \; L'(\eta)$$

where $X_o = \frac{1}{3} \alpha \beta \; J_s^2$.

This is what Brown does in reference 2, together with a good deal of justification for the assumptions involved. Technical Report No. 8[3] was based on this work. A simple extension[4] requiring no further assumptions than the previously utilized reversibility concept gives the expression for the transverse reversible susceptibility:

$$\frac{X_{rt}}{X_o} = 3 \; \frac{L(\eta)}{\eta} \quad .$$

This model is admittedly very crude and unrealistic, but various arguments can be given to justify its use. These arguments are all based upon the realization that the intrinsic properties of a ferromagnetic material which determine its reversible behavior can be expressed in terms of an energy function.

This energy function has been derived using various models, all of which give similar results. Therefore, when one utilizes this energy expression, he is not really basing his results on the accuracy of the model.

This property is very useful from the standpoint of predicting the susceptibility-magnetization behavior but, conversely, it makes attempting to draw conclusions of a microscopic nature from macroscopic results quite formidable.

In an effort to resolve this dilemma and to put his equations on a more realistic basis, Brown,[5] in 1939, once again derived the above expression for X_{rp}; this time by extending previous work of Kondorsky.[6] This work assumed that the volume of the individual domains changes when an external field is applied.

The resulting magnetization is no longer due solely to a different number of domains aligned with components in the field direction, but is now due to a larger volume of the domains oriented with components in the direction of the field.

The two derivations can be compared to reversible susceptibility due to rotation or to Bloch wall movement. One might expect to be able to say something regarding the origin of the initial susceptibility.[7,8] However, the statistical theory with isotropic material and a constant domain size is equivalent to assuming domain rotation. Brown's second paper assuming volume differences is equivalent to assuming wall movement. The results are the same, so no conclusions can be drawn.

The second theory does have the advantage that one can understand much more clearly the physical meaning of the assumptions involved. It would seem, therefore, that any attempt to extend this theory to large enough values of H so that irreversible jumps play a major role in the susceptibility should be based upon the second theory.

Reversible susceptibility data is presently being taken on three ferrite cores as a function of magnetization and temperature. We have recently found, since the arrival of the G.E. fluxmeter, a discrepancy in our measurements. Therefore, we haven't as much data as anticipated. The new data is presented in Figs. 1 and 2.* The necessary equipment for acquiring the data is now all here except the refrigerator. A technical report will be issued as soon as the data are all taken and analyzed.

3.1.2 B-H Loop Measurement. The G.E. fluxmeter arrived during the quarter. The 60-cycle B-H loop was checked against the dc loop. A comparison is

---

* These data and those in Figs. 3 and 4 were taken by Mr. J. D. Newton and Mr. R. M. Olson.

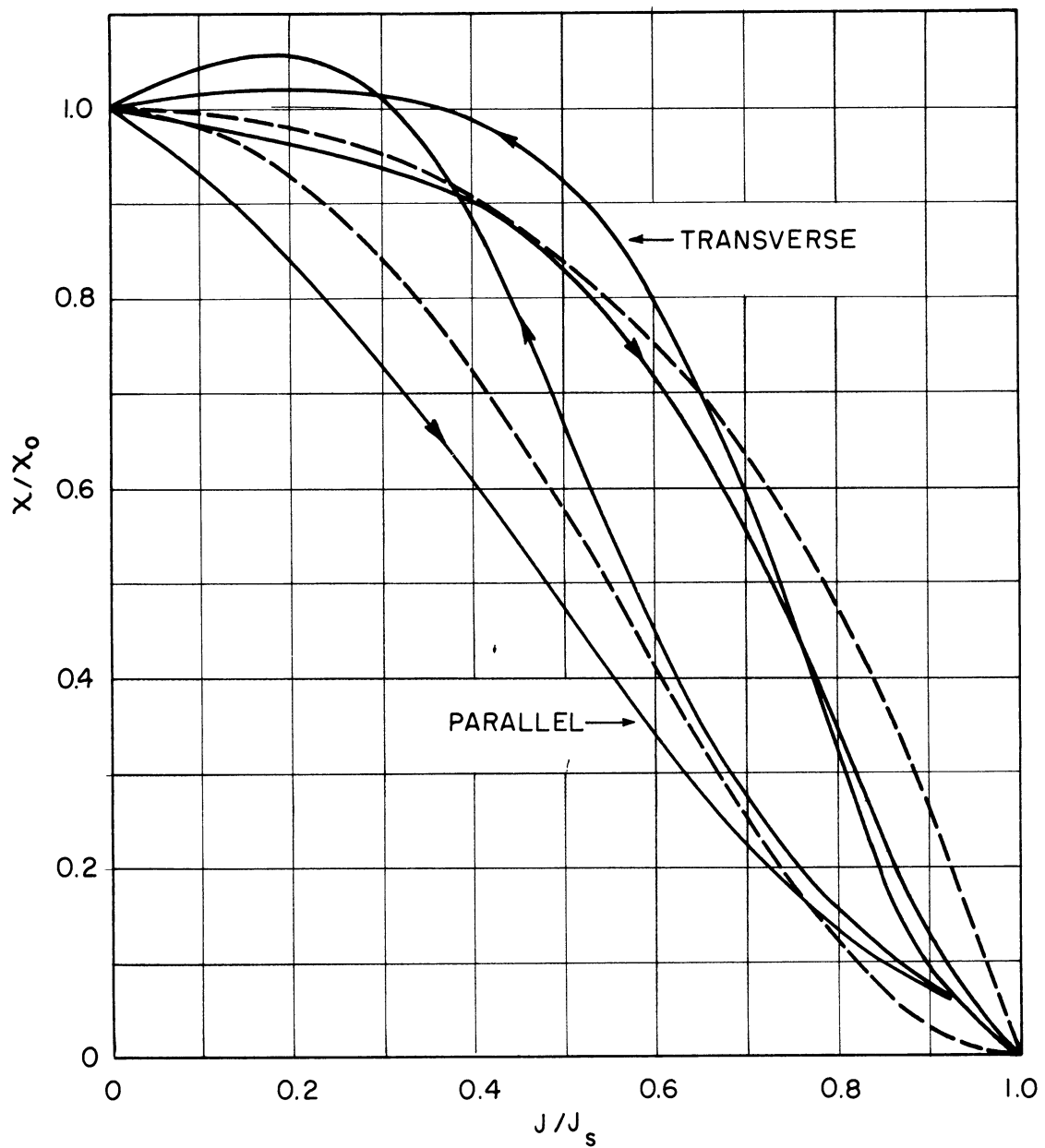FIG. I

GC-G-5
T = 25°C
J_s = 213 GAUSS, X_0 = 32.6

REVERSIBLE SUSCEPTIBILITY AS A FUNCTION OF MAGNETIZATION

———————————— EXPERIMENTAL VALUES
————————————— THEORETICAL VALUES

6

FIG. 2

GC-I-8
T = 25°C
J_s = 213 GAUSS, X_0 = 32.6

REVERSIBLE SUSCEPTIBILITY AS A FUNCTION OF MAGNETIZATION

——————————— EXPERIMENTAL VALUES
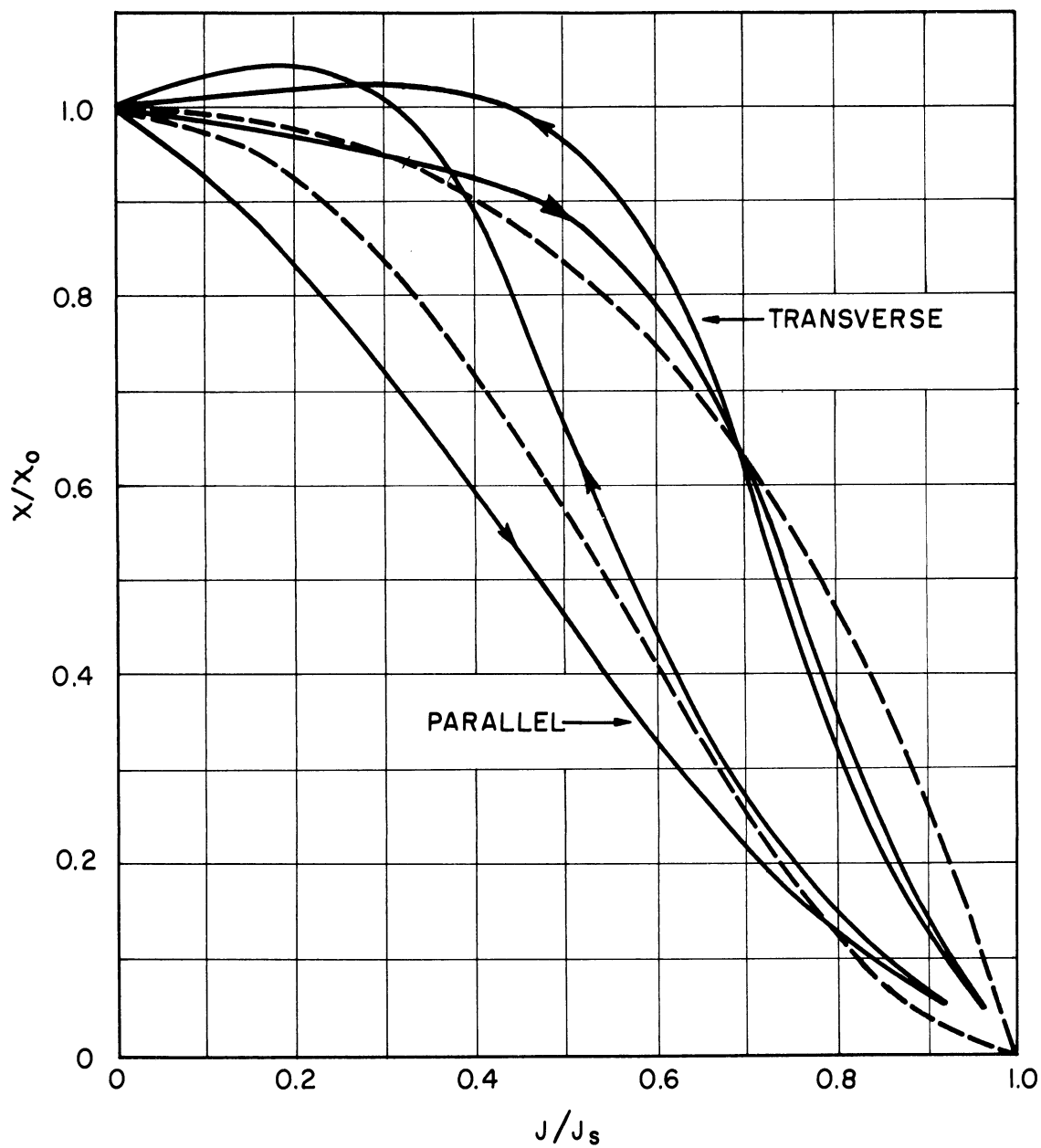
— — — — — — — — THEORETICAL VALUES

shown in Figs. 3 and 4. The coercive force is about 2 1/2 times as large on **one** 60-cycle loop as on the dc loop. The reason for this deviation is not clear. A small error in phase of the 60-cycle plotter would produce a large change in the coercive force. A magnetic mechanism sufficiently large to cause this difference is difficult to imagine. The problem was mentioned to Dr. G. T. Rado of the Naval Research Laboratories during the Durham meeting. He stated that because of the extreme error in the coercive force due to difference in phase, they take all their measurements using a dc method.

Because of these difficulties all B-H loops are now being taken using the dc method.

3.1.3 Parallel Reversible Permeability. Because of the difficulties encountered in B-H loop measurements, the μ_{rp} measurements are now being taken using a dc method. This circuit, designed by Dr. L. W. Orr, is shown in Fig. 5. The biasing field is adjusted by the potentiometer. The 4 henry choke is to present a high impedance to the alternating field on the dc side. It has been found experimentally that the circuit as now used has an upper frequency limit of about 10 kc. With minor alterations it could probably be used at a higher frequency if desired.

If one assumes a small enough ΔH so that a linear relationship exists between ΔB and ΔH, equivalent to the reversibility assumption, it follows simply that the reversible permeability is given by:

$$\mu_{rp} = \frac{\Delta B}{\Delta H} = \frac{5 \cdot 10^8 \; \bar{r}}{\omega \, AN_2^2} \; \frac{E_2}{E_1} \; R \qquad (1)$$

where

N_2 = number of turns on the B winding

E_2 = voltage drop across B winding

HBIAS (MAX) = 11.17 oe
T = 25°C

- - - - - D.C. LOOP
————— 60 ~ LOOP

B (GAUSS)

3000

2000

1000

-10   -5   5   10
HBIAS (OERSTEDS)

-1000

-2000

-3000

B

1000

HBIAS

-1   1

-1000

FIG. 3

GC-G-5

B-H LOOPS

9

T = 25°C
HBIAS (MAX) = 11.54 oe

- - - - D.C.LOOP
——— 60~LOOP

B (GAUSS)

2000

1000

-10   -5   5   10
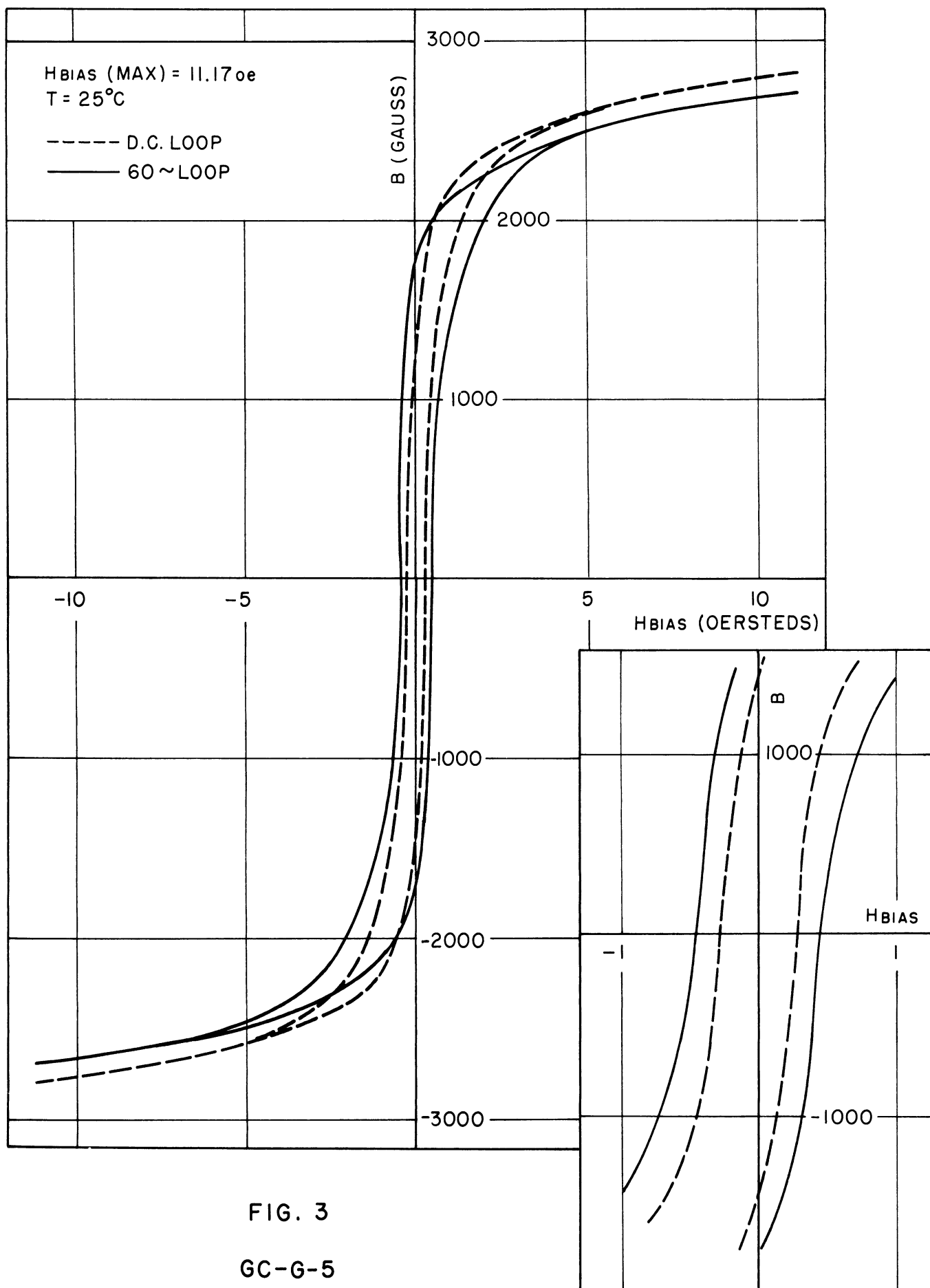
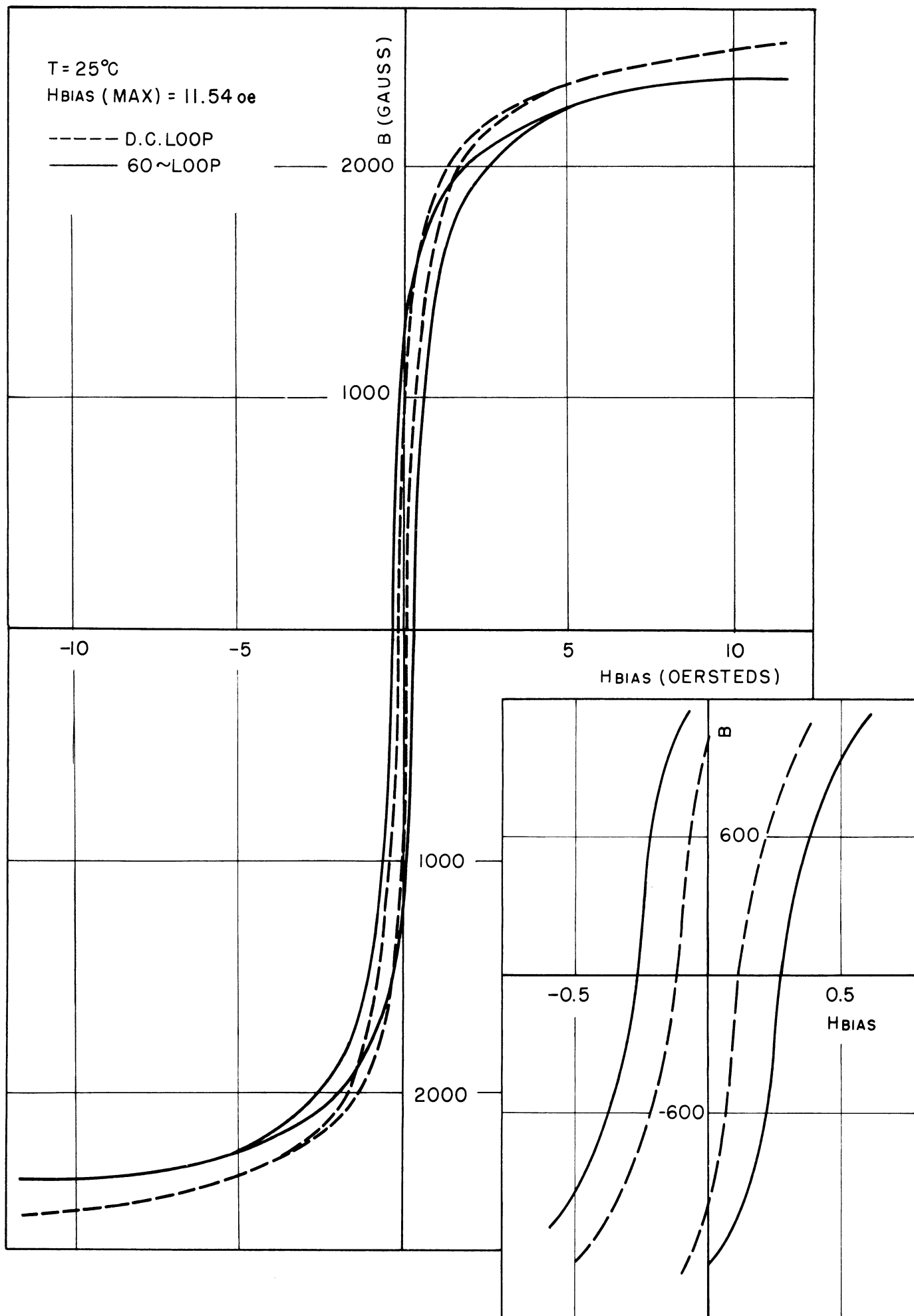HBIAS (OERSTEDS)

1000

2000

B

600

-0.5   0.5
HBIAS

-600

FIG. 4

GC-I-8, B-H LOOPS

E_1 = voltage drop across R box

$\bar{r}$ = mean magnetic radius of the core

A = cross-sectional area of the core

ω = radian frequency of the AC signal

R = resistance of the R box

3.1.4 Transverse Reversible Susceptibility. To obtain dc transverse measurements, the circuit described in the previous progress report is being altered as follows:

A dc source is applied to the magnet. The induction in the material is measured with the G.E. fluxmeter. The permeability is measured with the ac circuit of Fig. 5. Eq. (1) is once again applicable.

3.2 Manufacture of the Ferrites (D. W. Martin, L. Thomassen, B. Hershenov, D. M. Grimes)

3.2.1 Manufacturing Equipment.

Oven - The oven described in the previous progress report is still in use. This oven cannot reach temperatures much above 1350°C. The thermostatic temperature control has been improved and is nearly good enough, i.e., within ± 10°C at the highest temperatures, but is very poor at lower temperatures. Even more troublesome is the fact that the oven volume over which the temperature could be considered to be uniform is very limited, which keeps the batch sizes small. A search is still in progress to obtain a more satisfactory oven.

Pressing Dies - A second type of die has been designed for the manufacturer of rectangular cores for Hall Effect measurements (see Fig. 6). Considerable difficulty is met in trying to remove the pressed cores from the die without damage.

VTVM

DECADE
R BOX

470Ω 250 μμf

SIG.
GEN.

2

1

6

5

4HY
60ΩDC
250 MA

+ MA. − $R_M = 68Ω$

.28Ω .425Ω 2.125Ω 12Ω

0-25MA

250Ω

BATTERY
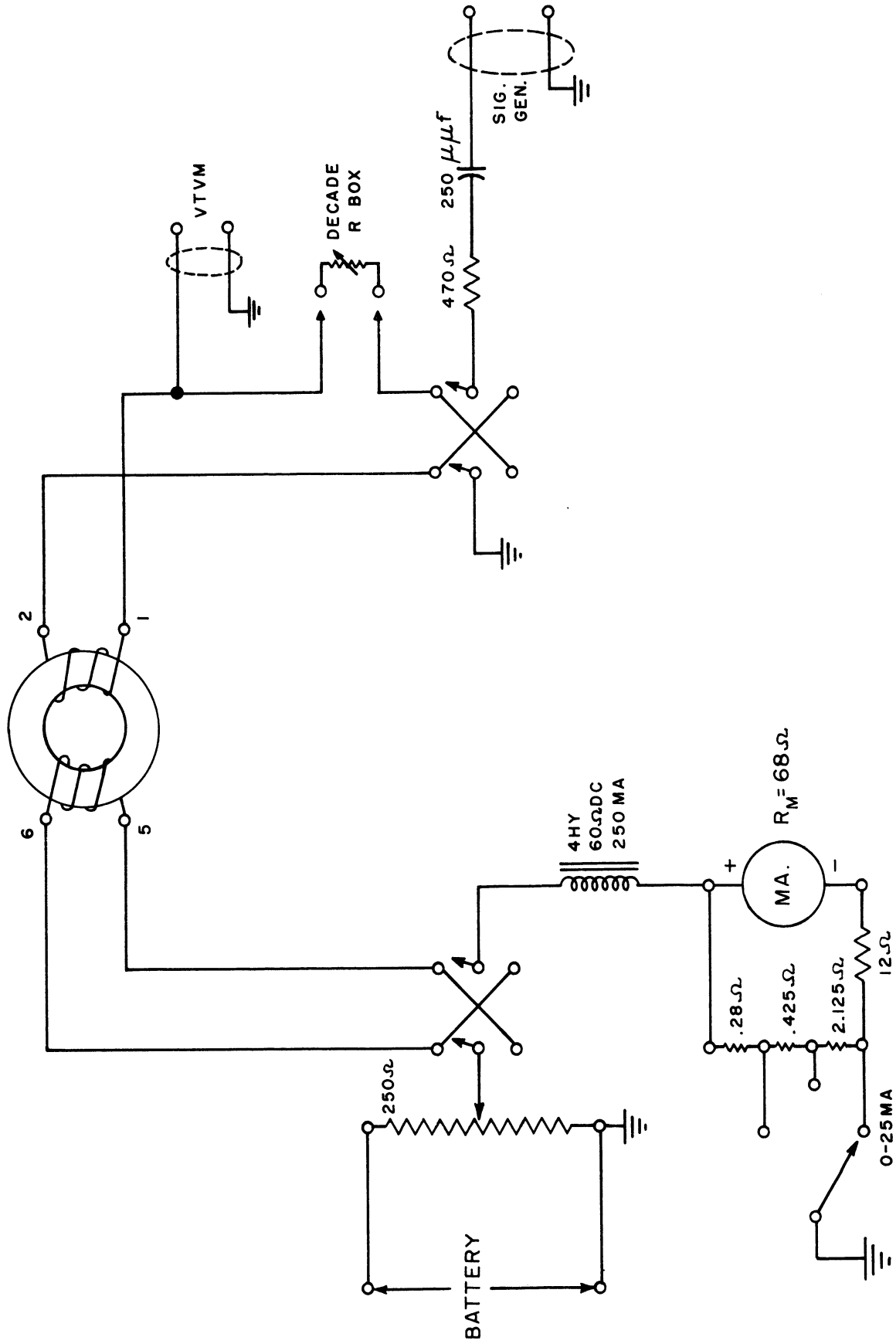
FIG. 5

CIRCUIT FOR PERMEABILITY MEASUREMENT.

12

PRESS →

(3)

(1)

FERRITE

(2)

RELEASE

(2)

(1)

FERRITE

(3)

PRESS ⟶

FERRITE PRESSING

RECTANGULAR DIE (TO SCALE)

FIG. 6

13

This same problem was resolved for the old style toroidal dies (see 1st Progress Report) by the construction of a jig provided with windings that make it an electromagnet (see Fig. 7). This jig holds the core rigidly in a plane perpendicular to the die axis, and supports it over a large part of the surface area as it is slid off the die. Then the core is held magnetically while being positioned over the firing boat, and released by shutting off the magnet.

3.2.2 Manufacturing Procedures.

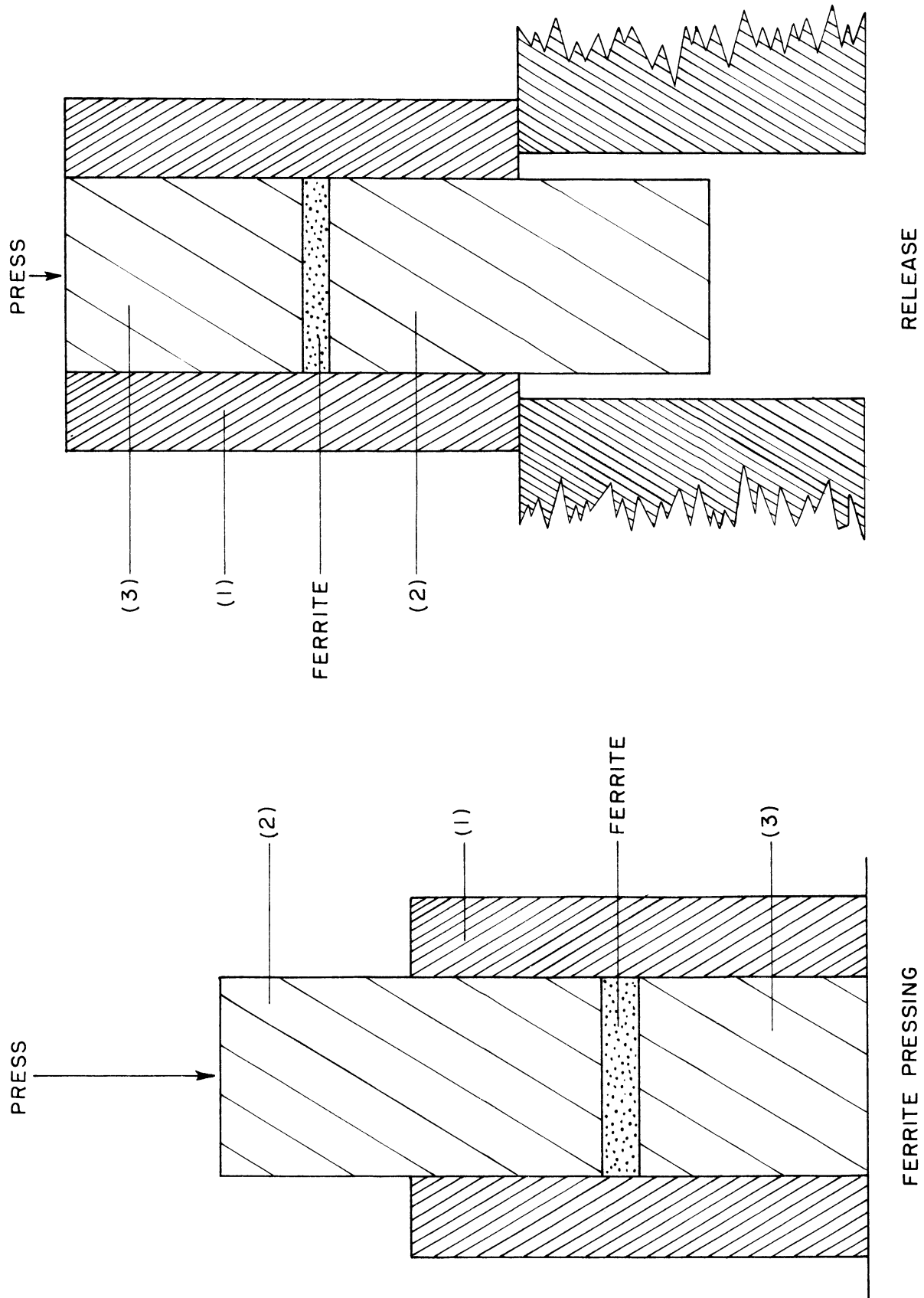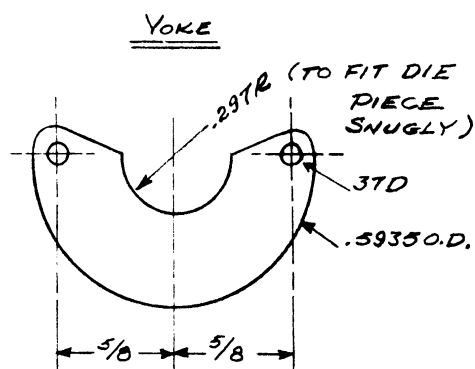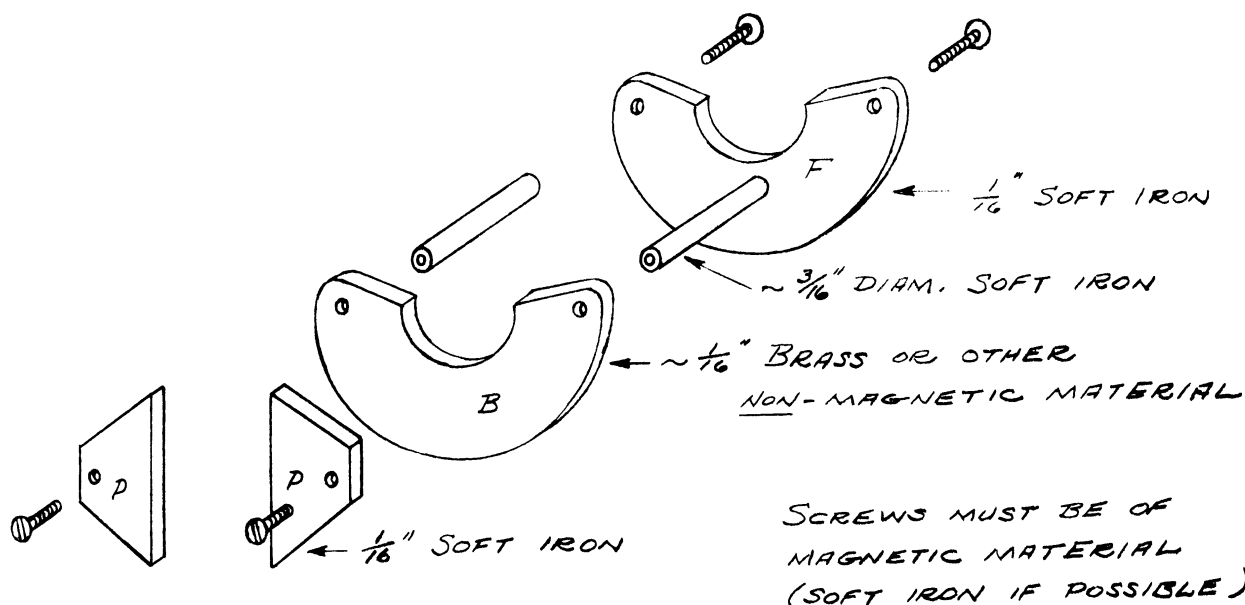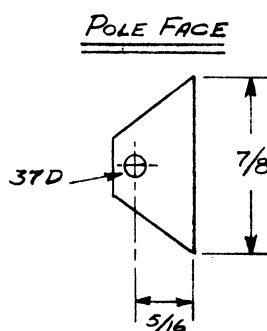Preliminary studies have clarified the problems involved and have pointed the way for future work. A number of cores have been produced under various sets of conditions with results ranging up to a quality comparable with commercial products. As yet, there has not been a large enough volume of production to permit independent evaluation of the many factors involved. However, a few conclusions have been reached, and the plans for further work are indicated below.

It is well known that ball milling of the oxide mixture causes a considerable impurity pickup. The use of iron mills is not a complete solution because excess iron will produce deviations from the desired composition. Microscopic examination of our raw materials shows no solid particles of size greater than the order of a micron, even though there are soft clumps of much larger size. Therefore, it is believed that something less drastic than grinding should be able to give the necessary homogeneity of the mixture.

Simple tumbling of the mixture in the mill without balls and with a large excess of water was tried. Many clumps were visible under the microscope and cores prepared from the mixture showed evidence of at least two phases (see Fig. 8). The second phase, presumably ZnO, is inside the circle. An additional difficulty was evident when a pyrex jar was used for the mill in that the heavier oxides, in this case CuO, could be seen to settle out appreciably faster from the

¼" SOFT IRON

~ 3/16" DIAM. SOFT IRON

F

~ 1/16" BRASS OR OTHER NON-MAGNETIC MATERIAL

B

P   P

¼" SOFT IRON

SCREWS MUST BE OF MAGNETIC MATERIAL (SOFT IRON IF POSSIBLE).

YOKE

.297R (TO FIT DIE PIECE SNUGLY)

37D

.5935 O.D.

5/8 5/8

TO BE 1/16" THICK.
MAKE 2:
    1 OF SOFT IRON (F)
    1 OF BRASS (B)

POLE FACE

37D

7/8

5/16

TO BE 1/16" THICK.
MAKE 2;
    SOFT IRON (P.P)

RODS

DRILL & TAP 3-48

9/16
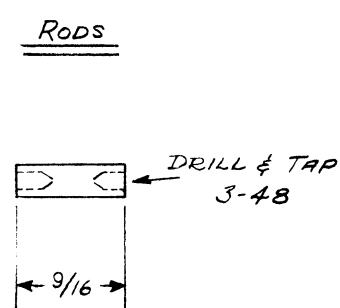
TO BE 3/16" DIAM.
MAKE 2:
    SOFT IRON

ASSEMBLY (TOP)

P →
B →

F →

DIE CENTER PUNCH →
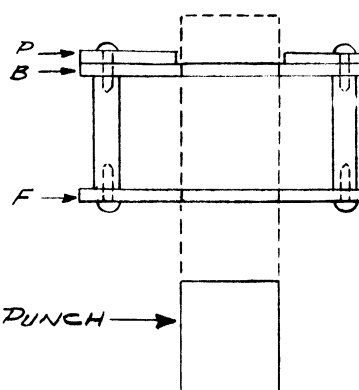
ALL DIMENSIONS UNLESS OTHERWISE SPECIFIED MUST BE HELD TO A TOLERANCE - FRACTIONAL ± 1/64," DECIMAL ± .005," ANGULAR ± ½°

		ENGINEERING RESEARCH INSTITUTE UNIVERSITY OF MICHIGAN ANN ARBOR MICHIGAN	DESIGNED BY	APPROVED BY
			DRAWN BY JEM	SCALE
			CHECKED BY	DATE 3-20-53
		PROJECT M-970	TITLE FIG. 7 MAGNETIC CORE JIG	
		CLASSIFICATION	DWG. NO. A-DT-115	
ISSUE	DATE			
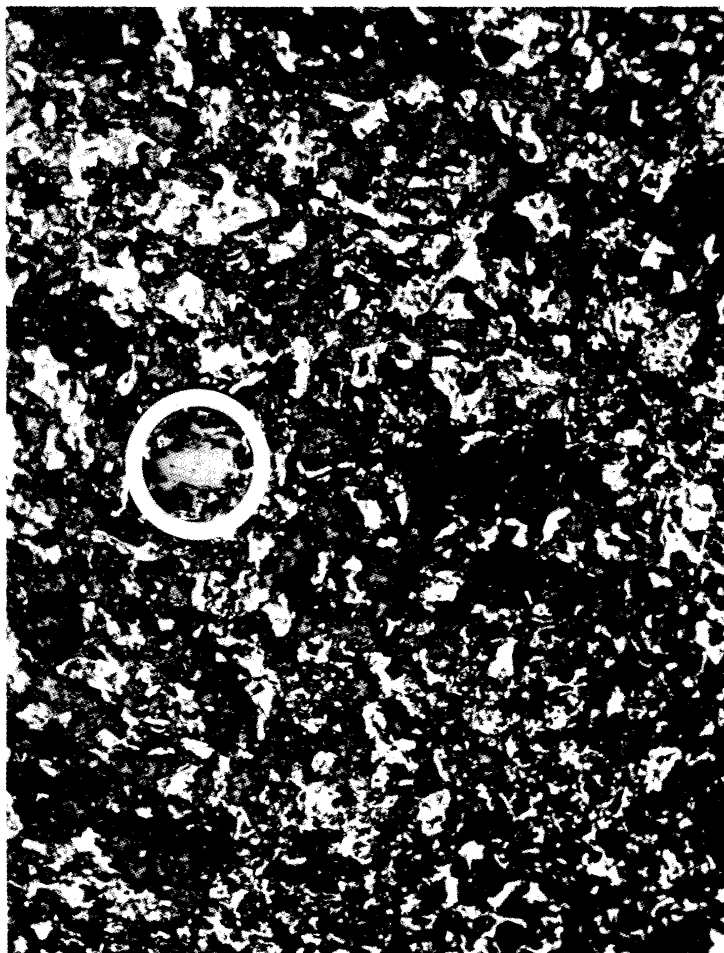
FIG. 8

TWO PHASE PHOTOGRAPH.

dilute slurry as soon as agitation ceased, leading to a gross variation of composition of the filtrate.

An attempt was made to effect mixing by energetic vibration of both dry mixtures and water slurries at audio frequencies. This technique seems unable to break up the clumps at all, and has been abandoned as impractical.

Present plans call for obtaining a high speed mixer which will be used with a baffle system to give violent agitation of a water slurry. This mixer, possibly supplemented by the use of a wetting agent, is expected to give intimate mixing with little contamination.

As in other laboratories, the ferrites are sintered and crushed at least once before being pressed for firing in the final form. Tests are contemplated to determine the relative advantages of having the ferrites in a loose porous state or pressed into a compact mass for this prefiring.

Crushing of the ferrite after the sintering operation is accomplished with a "diamond mortar" made of case-hardened steel. The grinding is brought about by compressive impact loading which utilizes the brittleness of the ferrite. Thus, the shear stresses involved in ordinary abrasive grinding techniques, with the accompanying introduction of impurities, are largely avoided.

The crushed ferrite has been passed through a 200 mesh sieve. Further check indicates that anywhere from 1/3 to 1/6 of this material would also pass through a 325 mesh. One batch was prepared of which about half was required to pass through only 50 mesh, the rest through 200 mesh. Specimens pressed from this coarser mixture were found to have better mechanical bonding prior to final firing. However, the best choice of particle size must be determined by the over-all electromagnetic properties desired.

Plans have been made to make routine quantitative chemical analysis in order that the effects of such factors as firing temperatures, times, atmospheres,

etc., may be directly evaluated in terms of the resulting oxygen content. It is hoped that the effects of the composition on the electromagnetic properties can thus be separated from effects of other factors such as grain size, etc., and will allow more systematic progress.

The dependence of these basic properties will in turn be correlated with the actual production control factors, a partial list of which includes:

1. firing temperature

2. length of time at firing temperature

3. heating rate

4. cooling rate

5. oven atmosphere

6. prefire time and temperature

7. moisture content of constituent oxides used in the sintering process

8. composition variation with respect to stoichiometric composition

Final evaluation of this data will involve a synthesis of the separate results. The composite result should yield a manufacturing technique for production of ferrites with the desired properties.

This exhaustive study will initially be applied to one ferrite, but many of the conclusions should be applicable to other compositions.

3.3 Specific Heat of Ferrite Materials (D. M. Grimes, E. Katz, E. F. Westrum, Jr.)

3.3.1 Theoretical Considerations. Assuming the sublattice picture of a ferrite as described originally by Neel,[9] and extended by Yafet and Kittel,[10] there are three possible types of transitions:

(1) Paramagnetic-Ferrimagnetic

(2) Antiferromagnetic-Ferrimagnetic or Triangular

(3) Ferrimagnetic-Triangular

Specific heat discontinuities should occur at each of these transition points. In the first two there is a discontinuity in the magnitude of the magnetization, in the third a discontinuity in the derivative of the magnetization with temperature.

The specific heat discontinuity in the three cases are:

(1) Paramagnetic-Ferrimagnetic transitions.[11]

$$\Delta C = \frac{2\lambda\mu \left[a^2 + 4\lambda\mu \right]}{a^2 + 2\lambda\mu + \dfrac{(\lambda - \mu)a}{\sqrt{a^2 + 4\lambda\mu}}} \Delta C_o$$

where: $\Delta C_o = 5NkS \dfrac{(S + 1)}{\left[(S + 1)^2 + S^2 \right]}$

$a = \lambda\alpha - \mu\beta$

S is the effective spin of the magnetic ion.

The other symbols are the same as used by Neel.

(2) Antiferromagnetic-Ferrimagnetic transitions.[12]

$$\Delta C = \frac{A^2}{2B} k$$

where: k is the Boltzman constant.

$$A = \frac{S + 1}{3S}$$

$$B = \frac{\left[(S + 1)^2 + S^2 \right] (S + 1)}{90 S^3}$$

(3) Ferrimagnetic-Triangular transitions.[12], *

$$\Delta C = -\frac{n}{\rho} \frac{M_a M_b}{uvT} \left[v\left(\frac{2}{p} - \gamma_2 \right) + u\left(\frac{2}{q} - \frac{1}{\gamma_2} \right) - 2\frac{u^2 + v^2}{uv - pv - qu} \right]$$

---

* This equation was derived by the authors. Later, a letter from Yafet indicates the same type of derivation.

$$\text{where:} \quad q = \frac{2\gamma_2}{\gamma_1 - \gamma_2}$$

$$p = \frac{2/\gamma_2}{\alpha_1 + \alpha_2 - 1/\gamma_2}$$

$$u = \left[\frac{d \log B_j \left(\frac{g\beta n}{kT} M_a \left[\alpha_1 + \alpha_2 - \frac{2}{\gamma_2} \right] \right)}{d \log \left(\frac{g\beta n}{kT} M_a \left[\alpha_1 + \alpha_2 - \frac{2}{\gamma_2} \right] \right)} \right]^{-1} - 1$$

$$v = \left[\frac{d \log B_j \left(\frac{g\beta n}{kT} M_b \left[\gamma_1 - \gamma_2 \right] \right)}{d \log \left(\frac{g\beta n}{kT} M_b \left[\gamma_1 - \gamma_2 \right] \right)} \right]^{-1} - 1$$

Both u and v are to be evaluated at the transition temperature. The other symbols are the same as used by Neel and by Yafet and Kittel. According to calculations that Yafet was kind enough to make,[12] the triangular-ferrimagnetic transitions should occur around 44°K and 377°K. The numbers were obtained for a ferrite of:

20 mole % NiO

30 mole % ZnO

50 mole % Fe_2O_3

The constants concerned were obtained from extrapolated paramagnetic data. As pointed out by Dr. Yafet, these estimates are at best only rough guides to the transition temperatures.

The theoretical basis for transitions of type (3) is now being reconsidered by the authors. The reason for this reconsideration is based upon the minimum energy condition at a temperature different from 0°K.

Using the model of Yafet and Kittel, the energy of the material due to magnetization of the four sublattices is:

$$E = -\sum_i \int_0^{M_i} \vec{H}_{\ell_i} \cdot d\vec{M}_i$$

$$E = -n \int_0^{M_{a'}} (\alpha_1 \vec{M}_{a'} + \alpha_2 \vec{M}_{a''} - \vec{M}_{b'} - \vec{M}_{b''}) \cdot d\vec{M}_{a'}$$

$$-n \int_0^{M_{a''}} (\alpha_2 \vec{M}_{a'} + \alpha_1 \vec{M}_{a''} - \vec{M}_{b'} - \vec{M}_{b''}) \cdot d\vec{M}_{a''}$$

$$-n \int_0^{M_{b'}} (-\vec{M}_{a'} - \vec{M}_{a''} + \gamma_1 \vec{M}_{b'} + \gamma_2 \vec{M}_{b''}) \cdot d\vec{M}_{b'}$$

$$-n \int_0^{M_{b''}} (-\vec{M}_{a'} - \vec{M}_{a''} + \gamma_2 \vec{M}_{b'} + \gamma_1 \vec{M}_{b''}) \cdot d\vec{M}_{b''}$$

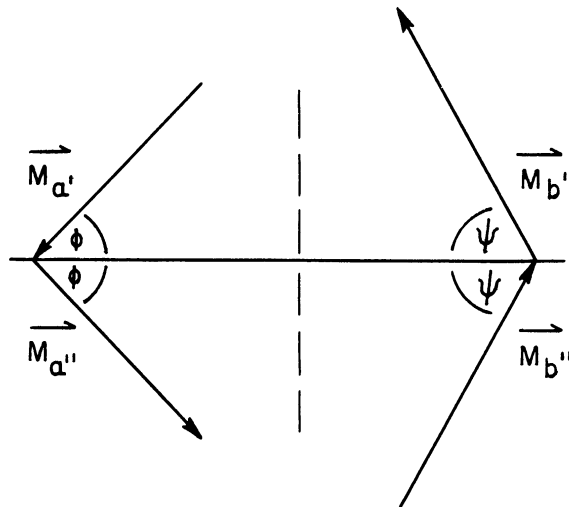where the symbols are the same as used by Yafet and Kittel. We now define:

$$\left| \vec{M}_{a'} \right| = \left| \vec{M}_{a''} \right| = M_a$$

$$\left| \vec{M}_{b'} \right| = \left| \vec{M}_{b''} \right| = M_b$$

FIG. 9.

POSSIBLE TRIANGULAR
ARRANGEMENTS.

Upon writing the energy expression in scalar form, with the angles defined by Fig. 9, and simplifying:

$$E = -2n \left[\int_0^{M_a} \left\{ M_a(\alpha_1 - \alpha_2 \cos 2\phi) + M_b(2 \sin \phi \sin \psi) \right\} d M_a \right.$$

$$\left. + \int_0^{M_b} \left\{ M_a(2 \sin \phi \sin \psi) + M_b(\gamma_1 - \gamma_2 \cos 2\psi) \right\} d M_b \right]$$

To integrate this expression, one must note that the angles ϕ and ψ are constant throughout the volume and depend only on the ratio M_a/M_b. One must assume the two integrals are evaluated simultaneously and in such a way that the ratio M_a/M_b at all times remains constant. The angles can then be removed from under the integral sign.

Thus:

$$E = -n \left[(\alpha_1 - \alpha_2 \cos 2\phi) M_a^2 + (\gamma_1 - \gamma_2 \cos 2\psi) M_b^2 \right.$$

$$\left. + 4 \sin \phi \sin \psi M_a M_b \right]$$

At 0°K., this expression is the same as that given by Yafet and Kittel. Upon minimizing this expression at 0°K., the following inequalities are found to describe the energy condition:

1. If $\alpha_2 \gamma_2 > 1$, $\phi = \psi = 0$

    the doubly antiferromagnetic state.

2. If $\alpha_2 \gamma_2 < 1$, the lowest state will depend upon M_a/M_b.

    (a) For $0 < \dfrac{M_a}{M_b} < |\gamma_2|$, the solution is $\phi = \dfrac{\pi}{2}$, $\sin \psi = \dfrac{M_a}{|\gamma_2| M_b}$

    (b) For $|\gamma_2| < \dfrac{M_a}{M_b} < \dfrac{1}{\alpha_2}$; $\phi = \psi = \dfrac{\pi}{2}$.

(c) For $\dfrac{1}{|\alpha_2|} < \dfrac{M_a}{M_b}$, the solution is $\psi = \dfrac{\pi}{2}$; $\sin \phi = \dfrac{M_b}{|\alpha_2|M_a}$.

These results come directly from the paper of Yafet and Kittel.

They next proceed to obtain another set of inequalities to describe the various transition temperatures. Upon finding these new inequalities, they next show how to evaluate the transition temperatures.

These temperatures, and later estimates of specific heat discontinuities, are based upon the inequalities existing at 0°K. However, these inequalities are not valid above 0°K. It is not clear at the moment how large an error this will involve. The reason for the discrepancy is that the minimum energy condition is obtained by minimizing the energy with respect to angular variations at a given temperature. At 0°K., only the explicit angular dependence need be considered for all sublattices are magnetized to saturation. At a higher temperature the magnitudes of the individual magnetizations are also implicit functions of the angles. The additional terms are of the same type as those involved in the expression for the specific heat discontinuities.

Work is continuing in an attempt to evaluate this discrepancy and its effect upon the specific heat.

3.3.2 Experimental Measurements. An initial study in the endeavor to test the molecular field treatment of the magnetic properties of ferrites given by Yafet and Kittel[10] was made on a sample of Ferramic E obtained from the General Ceramics Company. The material was supplied in the form of a toroidal cylinder 2.535 inches long, .338 inches inside diameter, 1.230 inches outside diameter, and an apparent bulk density of 4.62 gm/cm^3. The samples were fractured with a hard chromium steel hammer and anvil to average linear dimensions of approximately a millimeter. A total of 203.454 grams (in vacuo) of Ferramic E from a single

sample was loaded into calorimeter W-5 and the heat capacity was measured by the usual high precision technique.

Calorimeter W-5 is represented in a schematic cross section in Fig. 10. The essential details of this gold-plated, vacuum tight, sample container with entrant thermometer-heater well may be ascertained by reference to the Figure legend and to section 4.57 of the Quarterly Progress Report No. 1, Task Order EDG-6. (The cryostat and manner of operation are also described in the same section.) The top of the calorimeter is soldered in place with low melting cerium-indium solder after inserting the sample. The calorimeter is then evacuated to a high vacuum and filled with helium gas purified over charcoal at liquid nitrogen temperatures to provide thermal conduction.

The analysis of fragments of the sample of Ferramic E was made by the National Spectrographic Laboratories, Inc. They report traces (i.e., amounts less than 0.01% by weight) of aluminum, bismuth, cobalt, antimony, chromium, lead, lithium, magnesium, manganese, silicon, silver, tin, titanium, vanadium, and zirconium; molybdenum was not detected; and the copper content was reported as less than 0.1%.

Quantitative chemical analysis on the material by the same laboratory indicated the following percentages by weight of the major components:

$$Ni \quad\quad 8.94 \pm 0.05\%$$

$$Zn \quad\quad 17.58 \pm 0.10\%$$

$$Fe \quad\quad 48.10 \pm 0.25\%$$

On the assumption that the balance of the material is entirely oxygen, the following proximate composition is indicated:

NiO	15.56%	FeO	25.91%
ZnO	27.48%	Fe_2O_3	31.05%

This yields an empirical chemical formula of the form:

$$\left[Ni_{0.384}\ Zn_{0.678}\ Fe^{+2}_{0.640} \right] Fe^{+3}_{1.532}\ O_4$$
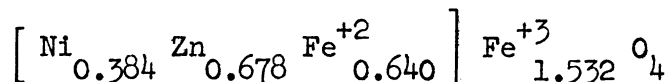
with a gram formula weight of 252.17. Assuming 20 mole % NiO, 30 mole % ZnO and

50 mole % Fe_2O_3, the ideal formula should read:

$$(Ni_{.40}\ Zn_{.60})\ Fe^{+3}_2\ O_4 \qquad .$$

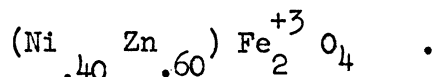It is evident, therefore, that even after taking account of the uncertainties of

the chemical analyses that the Ferramic E sample is deficient in oxygen compared

to a pure nickel-zinc ferrospinel.

The heat capacity data are presented in Table 1, both on per gram basis

and on the alternative basis of the gram formula weight calculated for Ferramic E

in terms of a defined thermochemical calorie equal to 4.1840 absolute joules.

These values of the heat capacity are believed to be accurate within 0.2% above

35°K with an uncertainty gradually increasing to about 0.5% at 20°K and to more

than a percent at the lowest temperatures. The determinations have been corrected

to true heat capacities with the exception that only the Series I runs have been

corrected for curvature. The data have been tabulated as C_s (heat capacity at

the equilibrium pressure of helium within the calorimeter); but since these pres-

sures are less than an atmosphere, the C_s values may be interpreted as virtually

identical with C_p (heat capacity at constant pressure).

The graph of the heat capacities as a function of temperature (Fig. 11)

reveals a very smooth curve with no scattering of the data whatever and no regions

of anomalous heat capacity between 5° and 308°K. This negative result cannot, of

course, be considered a test of the Yafet and Kittel predictions since the com-

position and magnetic properties, and therefore, possibly also the structure, do

not correspond to those of a ferrospinel lattice.

LEGEND FOR FIGURE 10.

1. THERMAL CONDUCTIVITY CONE.
2. MONEL HELIUM SEAL-OFF TUBE.
3. "LUBRISEAL" STOPCOCK GREASE.
4. COPPER VANE.
5. LEEDS AND NORTHRUP PLATINUM RESISTANCE THERMOMETER.
6. FIBREGLAS INSULATED #40 ADVANCE CONSTANTAN WIRE.
7. FORMVAR VARNISH.
8. GOLD PLATED COPPER HEATER WELL.
9. GOLD PLATED COPPER HEATER SLEEVE.
10. DIFFERENTIAL THERMO-COUPLE SLEEVE.
11. SPOOL TO BRING LEADS INTO THERMAL EQUILIBRIUM WITH CALORIMETER.

INSERT

3
4
5
6
7
8
9

4
8
9
10
5

INSERT

1

2

11

CM

5

4

3

2

1

0
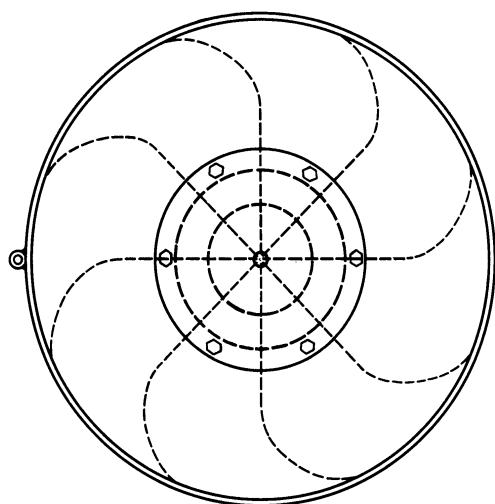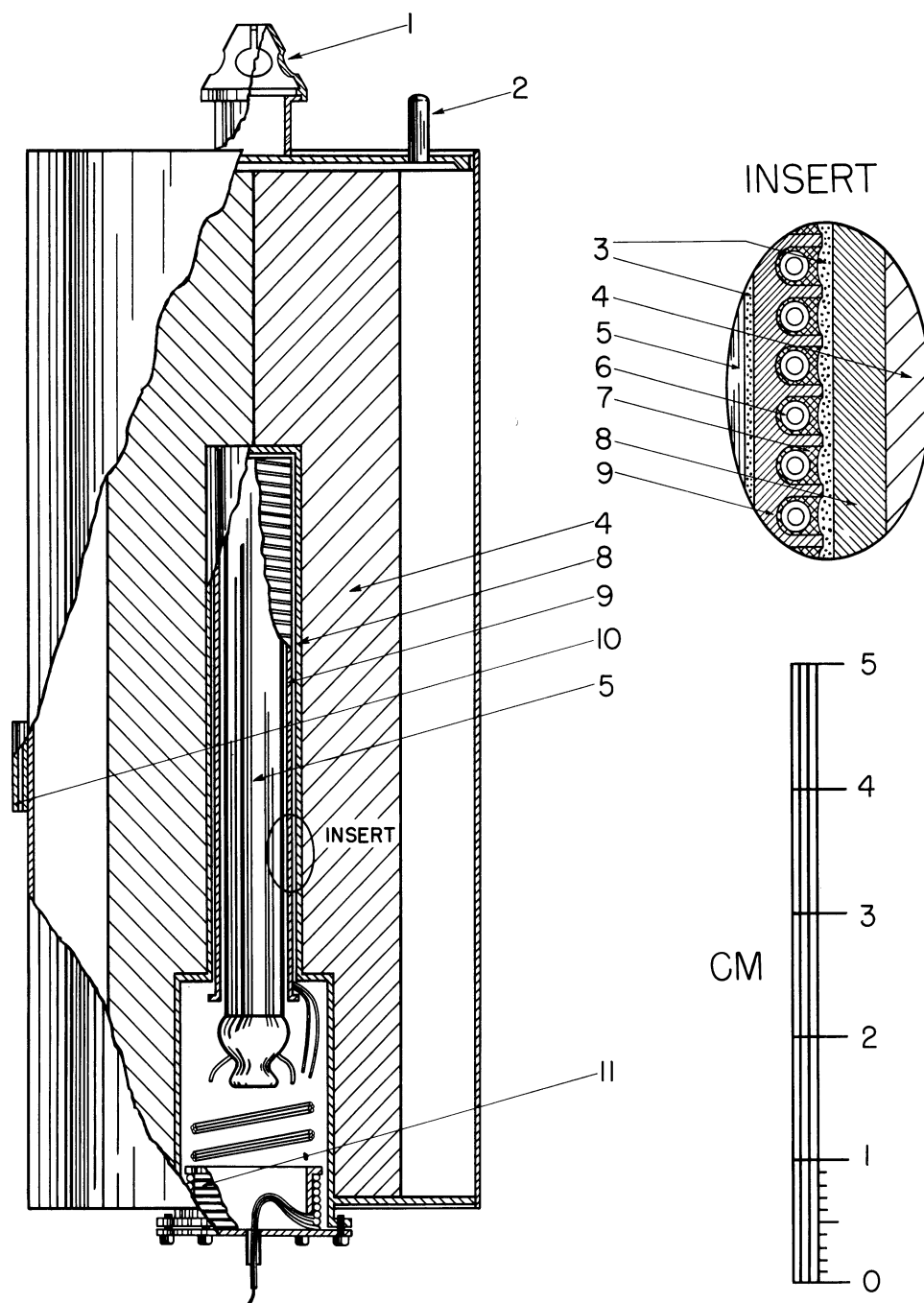
W-5 CALORIMETER

FIGURE 10

Table 1

Heat Capacity of Ferramic E

$$\left[Ni_{0.384}\ Zn_{0.678}\ Fe^{+2}_{0.640} \right] Fe^{+3}_{1.532}\ O_4$$
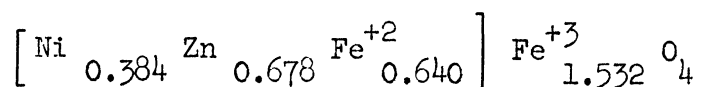
Gram Formula Weight = 252.17   0°C = 273.16°K

Series I

T °K	ΔT °K	C_s cal gm^{-1} deg^{-1}	C_s cal(gm form. wt.)$^{-1}$
5.59	0.655	.000364	0.092
6.36	1.016	.000404	0.102
7.38	1.297	.000564	0.142
8.65	1.360	.000816	0.206
10.00	1.551	.001074	0.271
11.45	1.547	.001292	0.326
12.94	1.496	.001501	0.379
14.46	1.570	.001755	0.443
16.04	1.614	.002051	0.517
17.72	1.740	.002350	0.593
19.54	1.908	.002739	0.691

Table 1
(Continued)

Series II

T °K	ΔT °K	C_s cal gm^{-1} deg^{-1}	C_s cal(gm form. wt.)$^{-1}$
16.78	1.796	.002189	0.552
18.64	1.925	.002568	0.648
20.61	2.026	.002996	0.756
22.80	2.348	.003572	0.901
25.27	2.587	.004323	1.090
27.97	2.821	.005277	1.331
30.95	3.132	.006353	1.602
34.11	3.179	.008148	2.056
37.47	3.547	.009774	2.465
41.26	4.030	.011934	3.009
45.54	4.517	.01457	3.674
50.25	4.904	.01768	4.458
55.23	5.060	.02109	5.318
52.74	4.412	.01937	4.885
57.47	5.038	.02267	5.717
63.00	6.017	.02673	6.741
69.23	6.446	.03125	7.880
75.89	6.880	.03621	9.131
83.03	7.382	.04165	10.50
90.35	7.266	.04724	11.91
97.86	7.760	.05280	13.32
105.87	8.254	.05870	14.80
114.12	8.242	.06472	16.32
122.47	8.449	.07065	17.82
131.20	9.022	.07679	19.36
140.13	8.830	.08276	20.87
149.01	8.932	.08851	22.32
158.03	9.112	.09407	23.72
167.25	9.324	.09947	25.08
168.47	8.930	.10013	25.25
177.45	9.021	.10508	26.50
186.57	9.209	.10982	27.69
195.75	9.155	.11432	28.83
204.81	8.976	.11858	29.90
213.75	8.884	.12249	30.89
222.67	8.963	.12618	31.82
231.62	8.932	.12974	32.72
240.59	9.014	.13310	33.56
249.57	8.954	.13636	34.39
258.62	9.156	.13933	35.14
267.81	9.213	.14223	35.87
276.99	9.155	.14508	36.59
286.10	9.087	.14755	37.21
295.17	9.062	.15019	37.87
304.24	9.075	.15252	38.46

LEGEND :

THE CIRCLES REPRESENT EXPERIMENTAL TRUE HEAT
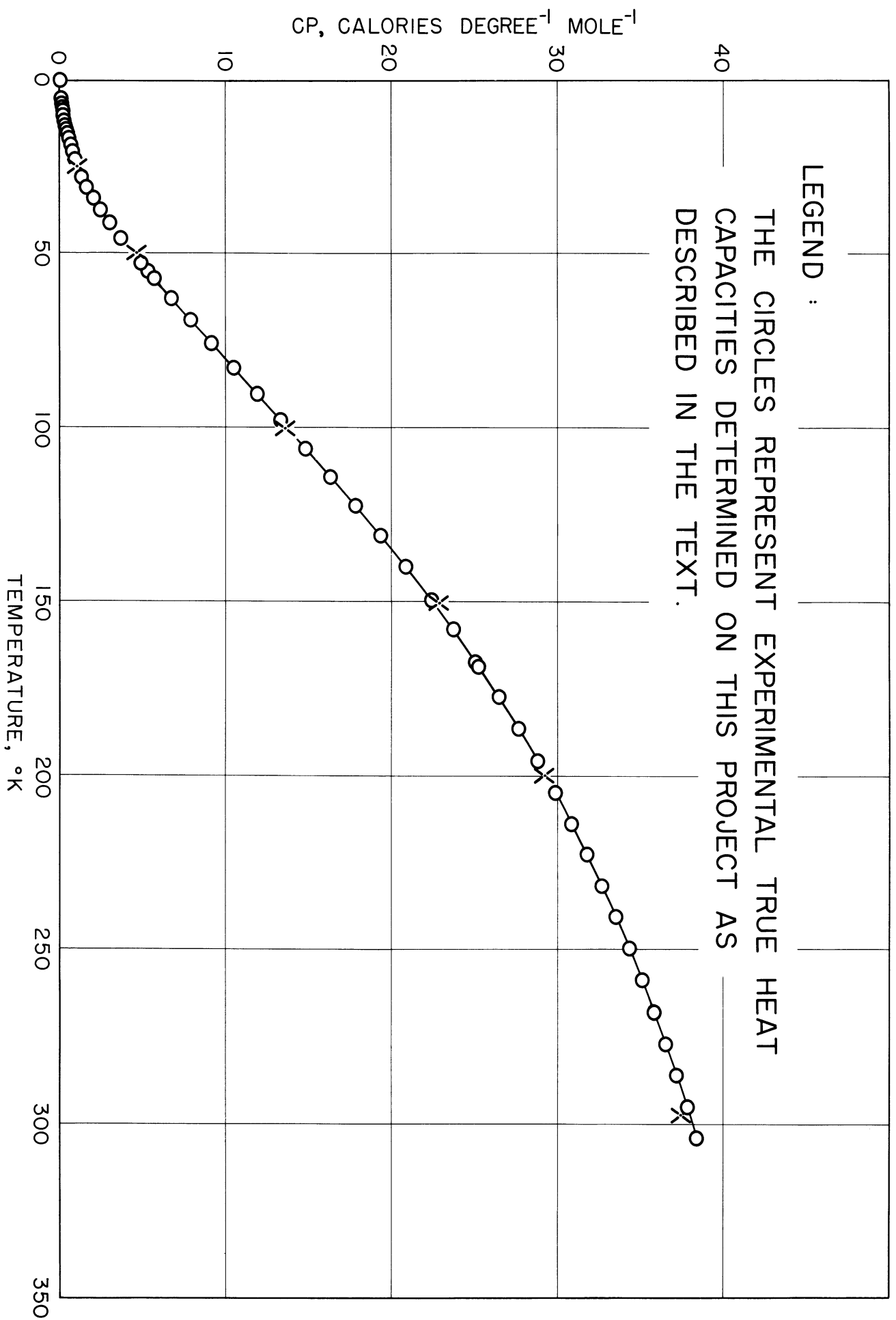CAPACITIES DETERMINED ON THIS PROJECT AS
DESCRIBED IN THE TEXT.

FIGURE II. THE HEAT CAPACITY OF FERRAMIC E.

It is interesting to note that the summation of the heat capacities of the constituent oxides (NiO, ZnO, FeO, and Fe_2O_3) multiplied by the appropriate factors yields a very good approximation to the measured heat capacity of Ferramic E except in the region of the anomaly in FeO. These summed points are represented by "X's" on Fig. 12. The heat capacities of the several oxides obtained from the literature are plotted in Fig. 12. The data were obtained from the following sources:

Zinc Oxide (ZnO): Crosses; Millar.[13] Open Circles; Maier,[14] et al.

Solid Dots; Clusius and Harteck.[15]

Nickel Oxide (NiO): Seltz,[16] et al.

Ferrous Oxide (FeO): Todd and Bonnickson.[17]

Ferric Oxide (Fe_2O_3): Parks and Kelley.[18]

It will be noted that the literature data are fragmentary and in poor agreement, so that the resultant summation of the heat capacity is at best an approximation.

3.4 Hall Effect. (B. Hershenov)

A rectangular die (see section 3.2.1) for manufacture of specimens for the Hall apparatus has been completed and used. No actual Hall measurements have been made because work has been directed toward the manufacture of suitable ferrite specimens. However, two nickel-zinc ferrite specimens have been prepared for measurement. The primary current leads are soldered to silver paint on the ends of the specimens. Quartz tubing will be used to press the Hall probes against the specimen. A specimen holder is being designed to constrain the specimen and avoid microphonics introduced by the 60 cps magnet. With the completion of the "holder" the entire apparatus will be recalibrated and a determination will be made of the Hall mobility, magneto-resistance, and the resistivity.
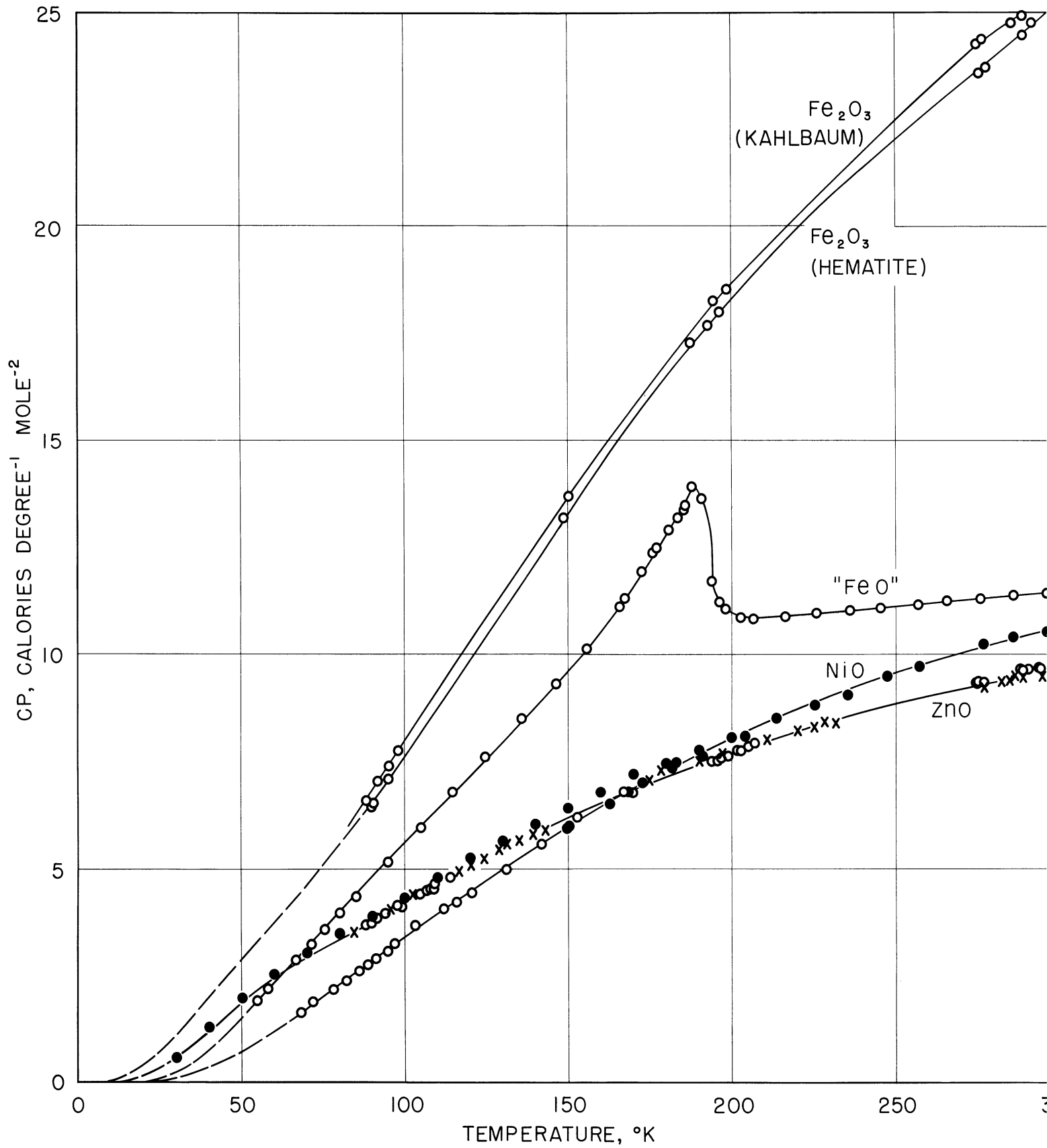
FIGURE 12.

THE HEAT CAPACITIES OF CERTAIN METAL OXIDES.

32

4. CONCLUSIONS (D. M. Grimes)

The most progress during the quarter was in acclimatizing the newly acquired personnel to the task at hand. Some of our equipment has arrived, some is still on order, and still other equipment has yet to be ordered.

In core manufacture, we have concluded that we can make our cores without the increased uncertainty due to an added binder. We have concluded that our mixing procedure was not satisfactory, and that an increased emphasis should be placed upon final quantitative analysis of the finished specimens.

We have decided that for the present we will strive for no higher chemical purity than can be obtained in commercial C.P. oxides.

5. PROGRAM FOR THE NEXT INTERVAL (D. M. Grimes)

5.1 Reversible Susceptibility

A technical report completing this work will be issued late in the quarter if no more obstacles arise. Data are being taken as rapidly as possible.

5.2 Core Manufacture

During the quarter oven equipment should arrive. At this time we will attempt to obtain a continuing supply of cores made under various controlled conditions.

The complex permeability and dielectric constant of each core will be systematically measured. We will attempt to correlate differences with manufacturing technique. These measurements are awaiting the arrival of measuring equipment promised by May 1.

It is hoped that a better idea of the desired physical properties which correlate with desired magnetic properties can be obtained from the sample cores furnished by the C.G.S. Laboratories.

5.3 Applicable Physical Measurements

It is hoped that sufficient specific heat data for a check of Yafet and Kittel's theory can be obtained. It is planned to also measure B_s over the same temperature range that the specific heat data is taken.

A new calorimeter capable of operating in the temperature range from room temperature to 300°C. is being built and should be completed during the quarter.

A satisfactory oven and mixing device will be available before the end of the quarter. A sample of the correct composition to show specific heat anomalies will be made as soon as possible. In the meantime, more accurate specific heat measurements on the constituent oxides will be made.

A suitable sample for Hall Coefficient measurement is now at hand. Work is now being directed toward the manufacture of a suitable sample holder. It is hoped that a trial run can be made before the end of the quarter.

REFERENCES

1. Gans, R., "Die Gleichung der Kurve der Reversiblen Suszeptibilitat," Physik. Z., 12, 1053, 1911.

2. Brown, William Fuller, Jr., "Domain Theory of Ferromagnetics Under Stress," Phys. Rev., 52, 325, 1937; Phys. Rev., 53, 428, 1938; Phys. Rev., 54, 279, 1938.

3. Grimes, D. M. "Theory of Reversible Magnetic Susceptibility with Application to Ferrites," Technical Report No. 8, Electronic Defense Group, August 1952.

4. Brown, William Fuller, Jr., Private correspondence.

5. Brown, William Fuller, Jr., "Theory of Reversible Magnetization in Ferromagnets," Phys. Rev., 55, 568, 1939.

6. Kondorsky, E. "On the Nature of Coercive Force and Irreversible Changes in Magnetization," Physik. Zeit. Sowjetunion, 11, 597, 1937; "The Magnetic Anisotropy of Ferromagnetic Crystals in Weak Fields: II. Theory of Reversible Susceptibility of Ferromagnetic Crystals," Compt. Rend. URSS, 19, 397, 1938.

7. Rado, G. T., Wright, R. W., and Emerson, W. H., "Ferromagnetism at Very High Frequencies: III. Two Mechanisms of Dispersion in a Ferrite," Phys. Rev., 80, 273, 1950; Rado, G. T., "Magnetic Spectra of Ferrites," Rev. Mod. Phys., 25, 81, 1953.

8. Went, J. J. and Wijn, H. P. J., "The Magnetization Process in Ferrites," Phys. Rev., 82, 269, 1951; Wijn, H. P. J. and Went, J. J., "The Magnetization Process in Ferrites," Physica, 17, 976, 1951; Polder, D. and Smit, J., "Resonance Phenomena in Ferrites," Rev. Mod. Phys., 25, 89, 1953; Wijn, H. P. J., Gevers, M. and Van der Burgt, C. M., "Note on the High Frequency Dispersion in Nickel Zinc Ferrites," Rev. Mod. Phys., 25, 91, 1953.

9. Neel, L., "Proprietes Magnetiques des Ferrites; Ferrimagnetisme et Antiferromagnetisme," Ann. Physique, 3, 137, 1948.

10. Yafet, Y. and Kittel, C., "Antiferromagnetic Arrangements in Ferrites," Phys. Rev., 87, 290, 1952.

11. Smart, J. Samuel, "The Specific Heat of Ferrites," Paper T2, American Physical Society, Cambridge Meeting, January 1953; and private correspondence.

12. Yafet, Y., Private correspondence.

13. Millar, R. W., "The Heat Capacity at Low Temperatures of Zinc Oxide and of Cadmium Oxide," Jour. Am. Chem. Soc., 50, 2653, 1928.

14. Maier, C. J., Parks, G. S., and Anderson, C. T., "The Free Energy of Formation of Zinc Oxide," Jour. Am. Chem. Soc., 48, 2564, 1926.

15. Clusius, K. and Harteck, P., "Uber die spezifischen Warmen einiger fester Korper bie tiefen Temperaturen," Zeit. Physik.-Chem., 134, 243, 1928.

16. Seltz, H., Dewitt, B. J., and McDonald, H. J., "The Heat Capacity of Nickel Oxide from 68° to 298°K and the Thermodynamic Properties of the Oxide," Jour. Am. Chem. Soc., 62, 88, 1940.

17. Todd, S. and Bonnickson, K. R., "Low Temperature Heat Capacities and Entropies at 298.16°K of Ferrous Oxide, Manganous Oxide, and Vanadium Monoxide," Jour. Am. Chem. Soc., 73, 3894, 1951.

18. Parks, G. S. and Kelley, K. K., "The Heat Capacities of Some Metal Oxides," Jour. Phys. Chem., 30, 47, 1926.

DISTRIBUTION LIST

Copy No. 1 Director, Electronic Research Laboratory
Stanford University
Stanford, California
Attn: Dean Fred Terman

Copy No. 2 Commanding Officer
Signal Corps Electronic Warfare Center
Fort Monmouth, New Jersey

Copy No. 3 Chief, Engineering and Technical Division
Office of the Chief Signal Officer
Department of the Army
Washington 25, D. C.
Attn: SIGGE-C

Copy No. 4 Chief, Plans and Operations Division
Office of the Chief Signal Officer
Washington 25, D. C.
Attn: SIGOP-5

Copy No. 5 Countermeasures Laboratory
Gilfillan Brothers, Inc.
1815 Venice Blvd.
Los Angeles 6, California

Copy No. 6 Commanding Officer
White Sands Signal Corps Agency
White Sands Proving Ground
Las Cruces, New Mexico
Attn: SIGWS-CM

Copy No. 7 Signal Corps Resident Engineer
Project LOCUST
Sylvania Center
Bayside, L. I., New York
Attn: F. W. Morris, Jr.

Copy Nos. 8-82 Transportation Officer, SCEL
Evans Signal Laboratory
Building No. 42, Belmar, New Jersey

For - Signal Property Officer
Inspect at Destination
File No. 25052-PH-51-91(1443)

Copy No. 83   W. G. Dow, Professor
Dept. of Electrical Engineering
University of Michigan
Ann Arbor, Michigan

Copy No. 84   H. W. Welch, Jr.
Engineering Research Institute
University of Michigan
Ann Arbor, Michigan

Copy No. 85   Document Room
Willow Run Research Center
University of Michigan
Willow Run, Michigan

Copy Nos. 86-95   Electronic Defense Group Project File
University of Michigan
Ann Arbor, Michigan

Copy No. 96   Engineering Research Institute Project File
University of Michigan
Ann Arbor, Michigan